TABLE 2

	Most Fe-rich olivine core of larger crystals *	Most common olivine, cores of small crystals *	Quench border; average of ~1–2 μ rim *	Calculated equilibrium olivine, no Fe-loss *	Chromite included in olivine	Glass Average **	Glass range ** (7 analyses)	Bulk composition of sample after experiment†	Calculated equilibrium liquid. Starting composition minus [45% olivine ($Fo_{90.1}$) + 1% chromite]
	1	2	3	4	5	6	7	8	9
SiO_2	41.3	41.2	39.8	40.9	–	59.7	59.2 – 60.2	49.2	54.6
TiO_2	–	–	–	–	3.0	2.5	2.5 – 2.7	1.1	2.2
Al_2O_3	–	–	0.6	–	10.0	13.7	13.2 – 14.1	6.1	10.7
Fe_2O_3	–	–	–	–	–	–	–	–	1.5
FeO	8.2	6.8	14.5	9.7	14.0	4.6	4.4 – 4.8	6.2	6.9
MnO	–	–	–	0.1	–	–	–	0.1	0.2
MgO	50.4	52.0	45.9	49.3	9.0	4.6	3.9 – 5.3	30.1	11.9
CaO	0.1	0.1	–	0.1	–	12.7	12.4 – 13.1	5.4	9.4
Na_2O	–	–	–	–	–	1.4	1.1 – 1.6	0.8	1.9
K_2O	–	–	–	–	–	0.6	0.6	0.2	0.4
Cr_2O_3	–	–	–	–	64.0	0.4	0.2 – 1.4	0.7	0.1
P_2O_5	–	–	–	–	–	0.2	00.2– 0.3	–	–
(H_2O)	–	–	–	–	–	(11%	–	–	–
$\frac{100\ Mg}{Mg + \Sigma Fe}$	91.6	93.0	84.5	–	52	64	61 – 66	89.7	72
$\frac{100\ Mg}{Mg + Fe^{++}}$	91.6	93.0	84.5	90.1	–	–	–	–	75.5

Run conditions: 10 kb, 1200°C, 1 hr, $Ag_{50}Pd_{50}$ capsule. 100 Mg/(Mg + ΣFe) of sample after run: 89.7.

* Some large (~30 μ) olivine crystals show reverse zoning reflecting growth of the crystal prior to Fe-loss to the $Ag_{50}Pd_{50}$ capsule (column 8) and failure of the centres of crystals to readjust to equilibrium as the bulk composition changed. Outer parts of such crystals and centres of smaller (10 μ) crystals have compositions Fo_{93} (column 2) and are taken to be in equilibrium in the bulk composition of column 8. Analyses of the outermost 1–2 μ of crystals, after correction for partial admixture of glass and high TiO_2 (quench ilmenite?) in the analysed volume, show compositions averaging $Fo_{84.5}$, indicating the presence of thin shells of olivine quench outgrowth on the primary crystals (column 3).

** The glass composition was obtained using only data from analyses in which the electron beam was moved over the areas of glass during analysis (100 sec). Data from stationary beam analyses, when corrected for low Na values, yield an almost identical average composition. In this and following tables glass compositions are recalculated to 100% anhydrous. The "H_2O" figure is estimated from the failure of the 11 elements determined to total to 100%, in contrast to totals of 98–101% for olivines and pyroxenes.

† Determined with 30 μ defocussed beam in continuous movement over polished surface of sample.

under the electron beam remove any uncertainty in correlating analytical data with petrographic observation.

To determine the effect of iron loss from the sample to the Ag–Pd capsule, bulk analyses of the samples were carried out using a defocussed (30 μ diameter) electron beam kept in continuous movement over the polished surface of the sample. The resultant analyses (e.g. table 2, column 8) gave excellent agreement with that of the initial mix (table 1, column 2) when corrected for Fe-loss, and thus provided a check on the analytical method. The data showed that there was appreciable iron loss from the 10 kb, 1200°C run (from 100 Mg/(Mg + ΣFe) = 85.2 to 89.7), slight iron loss from the 10 kb, 1100°C run, but no significant loss from 10 kb runs at $T < 1100$°C or in the 20 kb runs at $T \ll 1100$°C (see tables 2–12).

3. Experimental results

3.1. Water-saturated solidus

The experimental data are summarized in fig. 1 showing the results applied to pyrolite + 6% H_2O. The solidus is markedly depressed below the anhydrous solidus and is readily distinguished by textural change and the disappearance of phlogopite and amphibole at the beginning of melting at 30 kb and 20 kb respectively. At 10 kb the preferred solidus is shown as a solid line although the presence of rare, very low-R.I. glass and coarser grain size of the 970°C run relative to the 900°C run suggest that the solidus may lie at the lower-temperature dotted line. The glass at 970°C may however be quenched from the excess, intergranular vapour phase. Examination of the polished surface shows this vapour phase to be evenly distributed throughout the charge. Amphibole is an abundant phase in both the 900°C and 970°C runs accompanied by olivine and orthopyroxene and, at 970°C at least, by minor clinopyroxene *. There is no difference in Mg-value of orthopyroxene between the 900°C and 970°C runs so that the amount of melting at 970°C could only be very small. In addition, the Na/K, Ti/Na and Ti/K ratios of the amphibole at 970°C are close to those of the initial mix so that there are no chemical grounds from which to infer the existence of a low-melting fraction enriched in K, or Ti or Na, in addition to the solid phases at 970°C.

* The compositions and approximate proportions of olivine, orthopyroxene and amphibole also show that there should be another phase present in the pyrolite composition, with higher Ca : Al ratio than either orthopyroxene or amphibole.

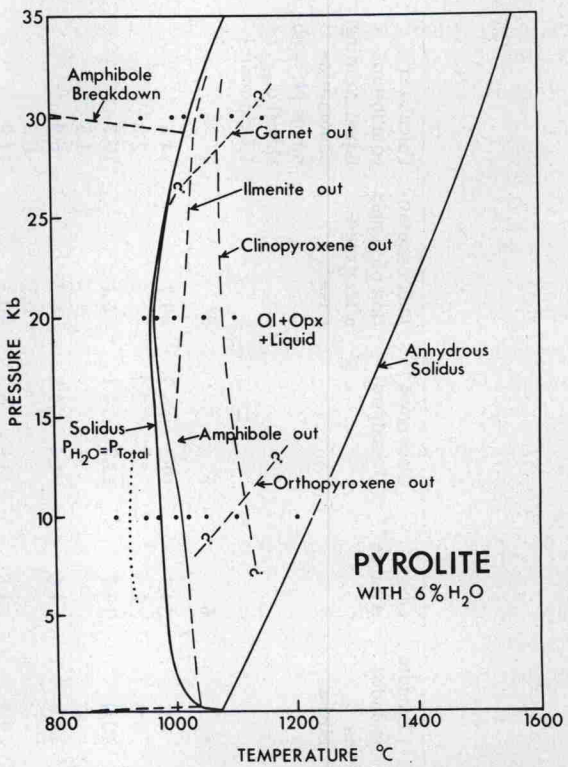

Fig. 1. Experimental determination of the water-saturated solidus for pyrolite composition. Experiments were carried out on (pyrolite minus 40% olivine) composition with 10% water added and data points are shown as black dots in the diagram. The subsolidus mineral assemblage at 10 kb and 20 kb is olivine + orthopyroxene + amphibole + clinopyroxene but at 30 kb the subsolidus assemblage is olivine + orthopyroxene + garnet + clinopyroxene + phlogopite + titanoclinohumite + ilmenite. The disappearance of major phases above the solidus is also shown. The anhydrous solidus is from ref. [6].

There are minor differences between the amphibole, considered to be subsolidus, at 970°C and that at 1000°C, where a minor melt fraction is observed and is considered to have caused the decreased K content and increased Na/K and Ti/Na ratios of the amphibole. The marked difference in Cr_2O_3 content of amphibole between 970°C and 1000°C is probably due to a tiny spinel inclusion in the 970°C amphibole, several other less satisfactory amphibole anlayses having about 1% Cr_2O_3. For the above reasons, the solidus at 10 kb is placed between 970°C and 1000°C and not at the lower-temperature dotted line of fig. 1. The order of disappearance of phases with increasing degree of melting is shown in fig. 1. There are minor